

THE RATE OF GROWTH OF VAPOR BUBBLES
IN SUPERHEATED WATER

Thesis by
Paul Dergarabedian

In Partial Fulfillment of the Requirements
For the Degree of
Doctor of Philosophy

California Institute of Technology
Pasadena, California

1952

ACKNOWLEDGMENTS

The writer wishes to thank Professor Milton S. Plesset for suggesting the investigation of the problem, and Mr. Albert T. Ellis for technical aid in setting up the high-speed photographic system.

This study was supported by the Shell Fellowship Committee and the Office of Naval Research.

ABSTRACT

Calculations are presented for the dynamic stability of vapor and air bubbles in superheated water. These calculations indicate that the values of the bubble radii for which the equilibrium is unstable are restricted to a finite range of radii whose values are governed by the temperature of the water and the initial air content in the bubble.

Two theoretical solutions for the rate of growth of these unstable bubbles are considered. The first, is a solution of the equation of motion of the bubble radius with the assumption that there is no heat diffusion across the bubble wall. The second, is a solution which includes the effect of heat diffusion. The two solutions differ appreciably.

These two solutions are then compared with the experimental data on the growth of the vapor bubbles in superheated water. This comparison shows agreement with the solution with the effect of heat diffusion included.

TABLE OF CONTENTS

Acknowledgements	i
Abstract	ii
Table of Contents	iii
I. Introduction	1
II. Theoretical Formulation of the Problem	4
1. Equation of Motion for the Growth of a Cavitation Bubble	4
2. Solution of Equation (6) Assuming $p_v = \text{Constant}$	6
3. Plesset-Zwick Theory for Bubble Growth	18
III. Apparatus and Procedure	23
1. Heating the Water	23
2. Temperature Measurements	26
3. Photographic Procedure	28
IV. Analysis of Data and Theory	31
1. Analysis of the Data	31
2. Comparison of Theory with Data	34
References	35
Figures	36

I. INTRODUCTION

One of the important problems in the field of hydrodynamics today, is the occurrence of cavitation in liquids. Cavitation is defined as the coexistence of a vapor or gas phase with the liquid phase. This vapor or gas phase first becomes evident in the form of bubbles distributed throughout the body of the liquid. Of practical significance is the increase in drag experienced by submerged bodies moving through a liquid when cavitation appears; similarly, pumps and turbines operate less efficiently in cavitating flow. The particular phase of the general field of cavitation presented in this paper is the fundamentally important problem of the dynamic stability and rate of growth of these vapor or gas bubbles.

Since the results in the present study are confined to the macroscopic behavior of the bubbles, it suffices to point out some of the present concepts concerning the initial formation of the bubble. The general view⁽¹⁾ is that bubble formation in cavitating flow, or in boiling, begins from a nucleus within the liquid containing air, or vapor, or both. These gas-phase nuclei are ordinarily submicroscopic in size, and become evident upon the growth of the nuclei through a temperature rise in the liquid or a reduction in the external pressure acting on the liquid.

In dealing with multiple-phase systems the important role of surface phenomena must be considered in the processes involved. Thus in the case of these submicroscopic nuclei the very large forces of

surface tension must be overcome to initiate cavitation or boiling. It is well known that degassed pure liquids can withstand very large tensions, or may be superheated considerably, without the formation of bubbles. This effect has been demonstrated by Harvey⁽²⁾ and subsequently by Pease and Blinks⁽³⁾. Harvey subjected samples of water saturated with air to pressures (of the order of 10,000 psi) for several minutes. In this manner, the air nuclei are squeezed into solution so that when the solution is brought back to atmospheric pressure it does not cavitate under the tensions which freely produced cavitation before the pressurization. These same pressure-treated air-water solutions also can be superheated by as much as 80°C without boiling.

For the case of ordinary untreated water the gas-phase nuclei may be stabilized on small solid particles. The presence of a solid, or third phase, is indicated since the surface energy of a bubble bounded by a solid surface and a liquid surface may be very low. Evidence for this condition can be found in the fact that the theoretical boiling point for pure water⁽⁴⁾ is much higher than the values obtained by any experiment on superheating of water.

Since the macroscopic behavior of the bubbles formed in a boiling liquid may be considered as entirely analogous to cavitation bubbles, the experiments and calculations in this paper describe the rate of growth of vapor bubbles in superheated water. In the case of boiling liquids by an increase in temperature, the effects upon heat transfer

rates due to the vapor phase are of great interest. The experimental part of this paper is an analysis of high-speed photographs of the growth of vapor bubbles at various degrees of superheat. For the theoretical phase, calculations are presented on the dynamic stability of vapor and air bubbles in order to determine equilibrium bubble radii for growth. In order to emphasize the important effect of cooling of the bubble wall during the growth, solutions of the equation of motion for the bubble radius are considered both with and without heat conduction across the bubble wall.

II. THEORETICAL FORMULATION OF THE PROBLEM

I. Equation of Motion for the Growth of a Cavitation Bubble

Frequent reference is made in the literature on cavitation to Rayleigh's solution for the problem of the collapse of a spherical cavity in a liquid⁽⁵⁾. Rayleigh's theory can be extended to the case for the growth of a bubble. Rayleigh considered the situation in which the pressure at a great distance from the bubble was constant. With this assumption, plus the assumption of an incompressible fluid, the variation of the bubble radius with time is obtained from the energy integral of the motion. For the present problem of the growth of a bubble the extension of the Rayleigh theory as carried out by Plesset⁽¹⁾ can be used to obtain the equation of motion. The equation is obtained by considering a spherical bubble in a perfect incompressible fluid of infinite extent. Neglecting the effects of gravity, the origin is chosen at the bubble center which is at rest. The radius of the bubble for any time t is R , and r is the radius to any point in the liquid. Thus the velocity potential for the liquid is expressed by

$$\varphi = \frac{R^2 \dot{R}}{r} \quad (1)$$

and the Bernoulli integral of the motion is

$$-\frac{\partial \varphi}{\partial t} + \frac{1}{2} (\nabla \varphi)^2 + \frac{p(r)}{\rho} = \frac{P(t)}{\rho} \quad (2)$$

with ρ constant and being the density of the fluid and

where $\dot{R} = \frac{dR}{dt}$, $p(r)$ is the static pressure at r , and $P(t)$ is the static pressure at a distance from the bubble. From Eq. (1)

$$(\nabla \varphi)^2 = \frac{R^4 \dot{R}^2}{r^4}, \quad (3)$$

$$\frac{\partial \varphi}{\partial t} = \frac{1}{r} (2R\dot{R}^2 + R^2\ddot{R}), \quad (4)$$

and applying Eq. (2) at $r = R$, the equation of motion for the bubble radius is obtained. Thus with

$$\left(\frac{\partial \varphi}{\partial t} \right)_{r=R} = 2\dot{R}^2 + R\ddot{R},$$

$$(\nabla \varphi)_{r=R}^2 = \dot{R}^2$$

Eq. (2) becomes

$$R\ddot{R} + \frac{3}{2}\dot{R}^2 = \frac{p(R) - P(t)}{\rho} \quad (5)$$

Equation (5) is the general equation of motion for a spherical bubble in a liquid with given external pressure $P(t)$, and with the pressure at the bubble boundary $p(R)$. Rayleigh's equation is obtained as a special case if

$$P(t) - p(R) = P_0 \text{ (a constant).}$$

Equation (5) is adapted to the present problem with the assumption that

$$p(R) = p_v + p_A - \frac{2\sigma}{R}$$

where p_v is the vapor pressure of the water at the appropriate temperature, p_A is the pressure of any air which may be in the bubble of radius R , and σ is the surface tension constant for water. Letting

$$P(t) = p_{\infty} \text{ (a constant)}$$

where p_{∞} is the atmospheric pressure, the equation of motion for the bubble radius becomes

$$R \ddot{R} + \frac{3}{2} \dot{R}^2 = \frac{p_v - p_{\infty} + p_A - \frac{2\sigma}{R}}{\rho} \quad (6)$$

2. Solution of Equation (6) Assuming $p_v = \text{Constant}$.

If the assumption is made that the vapor pressure p_v remains constant throughout the growth of the bubble, then the bubble growth is isothermal or

$$p_A = p_{A_0} \frac{R_0^3}{R^3} \quad (7)$$

where p_{A_0} is the initial pressure of the air in a bubble of radius R . Equation (7) implies the assumption that no air diffuses across the bubble boundary as it grows. Plesset and Epstein⁽⁶⁾ have shown that the diffusion process for gas bubbles is so slow compared to the rate of growth of the bubble that it does not effect the air content of the bubble. Thus Eq. (7) is a reasonable expression for the air pressure p_A as a function of the bubble radius.

From Eq. (6) it can be seen that the bubble is in dynamic equilibrium with the liquid if

$$\begin{aligned} f(R) &= p_v - p_{\infty} + p_{A_0} \frac{R_0^3}{R^3} - \frac{2\sigma}{R} = 0, \\ \dot{R} &= 0. \end{aligned} \quad (8)$$

One obvious root of Eq. (8) is $R = R_0$, where

$$R_0 = \frac{2\sigma}{p_v + p_{A_0} - p_{\infty}}.$$

The remaining roots of Eq. (8) are then found to be

$$R = \frac{p_{A_0} \sigma}{\delta p (\delta p + p_{A_0})} \left\{ 1 \pm \sqrt{1 + 4 \frac{\delta p}{p_{A_0}}} \right\},$$

where $\delta p = p_v - p_\infty$. If $\delta p > 0$, then the two positive roots of Eq. (8) which correspond to actual bubble radii are

$$R = \frac{2 \sigma}{\delta p + p_{A_0}}$$

and

$$R = \frac{p_{A_0} \sigma}{\delta p (\delta p + p_{A_0})} \left\{ 1 + \sqrt{1 + 4 \frac{\delta p}{p_{A_0}}} \right\}.$$

The case $\delta p > 0$, corresponds to the condition that the vapor pressure p_v , is greater than the atmospheric pressure p_∞ , so that the liquid can boil. If $\delta p \leq 0$, then there is only one positive root of Eq. (8), namely

$$R = \frac{2 \sigma}{\delta p + p_{A_0}}$$

provided that $p_{A_0} > |\delta p|$.

The effect of varying the value of the initial air pressure p_{A_0} on the equilibrium radii will be considered next.

For the case $\delta p > 0$, it should be noted that

$$p_{A_0} R^3 = p_{A_0} \left(\frac{2 \sigma}{\delta p + p_{A_0}} \right)^3$$

has the value zero for $p_{A_0} = 0$, and increases to a maximum value of

$$\frac{\delta p}{2} \left(\frac{4\sigma}{3\delta p} \right)^3, \quad p_{A_0} = \frac{\delta p}{2}$$

and then approaches zero as $p_{A_0} \rightarrow \infty$. Thus the entire range of values for $p_{A_0} R_0^3$ is covered in considering $0 \leq p_{A_0} \leq \frac{\delta p}{2}$. For the case of a vapor bubble, $p_{A_0} = 0$, and there is only one positive root for Eq. (8), its value being

$$R = \frac{2\sigma}{\delta p}.$$

When $p_{A_0} = \frac{\delta p}{2}$, the two positive roots coincide with a value of

$$R = \frac{4\sigma}{3\delta p}.$$

If any values of $p_{A_0} > \frac{\delta p}{2}$ are considered, the two roots merely interchange roles. Thus for the case $\frac{\delta p}{2} > 0$, it is sufficient to consider the two roots

$$R = R_0 = \frac{2\sigma}{\delta p + p_{A_0}}$$

for $0 \leq p_{A_0} \leq \frac{\delta p}{2}$, and

$$\begin{aligned} R = R_1 &= \frac{p_{A_0}\sigma}{\delta p(\delta p + p_{A_0})} \left\{ 1 + \sqrt{1 + 4 \frac{\delta p}{p_{A_0}}} \right\} \\ &= \frac{2\sigma}{\delta p + p_{A_1}} \end{aligned}$$

$$p_{A_1} = \frac{2\delta p(\delta p + p_{A_0})}{p_{A_0} \left\{ 1 + \sqrt{1 + 4 \frac{\delta p}{p_{A_0}}} \right\}} - \delta p$$

for $p_{A_1} > \frac{\delta p}{2}$. Thus the entire range of possible values for the initial air pressure in the bubble is covered. For the case

$\delta p \leq 0$, the only root is

$$R = R_o = \frac{2\sigma}{\delta p + p_{A_o}}$$

with $p_{A_o} > |\delta p|$.

To determine whether the equilibrium of a bubble is dynamically stable or unstable, one may consider

$$\frac{df(R)}{dR} = \frac{2\sigma}{R^2} - 3p_{A_o} \frac{R_o^3}{R^3} \quad (9)$$

for the given radius. Thus for dynamic stability, $\frac{df(R)}{dR} < 0$ and for dynamic instability, $\frac{df(R)}{dR} > 0$. For the case $\delta p > 0$ and radius

$$R = R_o = \frac{2\sigma}{\delta p + p_{A_o}} ,$$

Eq. (9) becomes

$$\left. \frac{df(R)}{dR} \right|_{R=R_o} = \frac{\delta p + p_{A_o}}{2\sigma} (\delta p - 2p_{A_o})$$

or

$$\left. \frac{df(R)}{dR} \right|_{R=R_o} \geq 0$$

if $0 \leq p_{A_o} \leq \frac{\delta p}{2}$. This means that the equilibrium of a bubble of radius $R_o = \frac{2\sigma}{\delta p + p_{A_o}}$, with $\delta p > 0$, is dynamically unstable if $0 \leq p_{A_o} < \frac{\delta p}{2}$. For the case $p_{A_o} = \frac{\delta p}{2}$, $\frac{df(R)}{dR} = 0$,

the bubble is dynamically unstable if the radius is increased beyond R_o but is dynamically stable if the radius is decreased below R_o . In terms of the growth of the bubble the range of equilibrium radii are

$$\frac{4\sigma}{3\delta p} \leq R_o \leq \frac{2\sigma}{\delta p}$$

with

$$\frac{\delta p}{2} \geq p_{A_o} \geq 0.$$

For the radius

$$R = R_1 = \frac{2\sigma}{\delta p + p_{A_1}} \quad , \quad p_{A_1} > \frac{\delta p}{2} \quad ,$$

Eq. (9) becomes

$$\left. \frac{df(R)}{dR} \right|_{R=R_1} = -3 p_{A_o} \frac{R_o^3}{R_1^4} + \frac{2\sigma}{R_1^2}.$$

Since $R_1 < R_o$ and $\left. \frac{df(R)}{dR} \right|_{R=R_o} = 0$ for $p_{A_o} = \frac{\delta p}{2}$,

one obtains

$$\left. \frac{df(R)}{dR} \right|_{R=R_1} < 0$$

for all $p_{A_1} > \frac{\delta p}{2}$. This means that all bubbles of radius

$R_1 < \frac{4\sigma}{3\delta p}$ with $\delta p > 0$, are dynamically stable. However, these bubbles soon dissolve through diffusion of air out of the bubble⁽⁶⁾.

For the case $\delta p \leq 0$, with $p_{A_o} > |\delta p|$, the equilibrium radius is

$$R_o = \frac{2\sigma}{\delta p + p_{A_o}} ,$$

and Eq. (9) becomes

$$\left. \frac{df(R)}{dR} \right]_{R=R_o} = \frac{\delta p + p_{A_o}}{2\sigma} (\delta p - 2p_{A_o}) .$$

Since $p_{A_o} > |\delta p|$, one obtains

$$\left. \frac{df(R)}{dR} \right]_{R=R_o} < 0 .$$

This means that if the vapor pressure p_v , is less than the atmospheric pressure p_∞ , then any air bubble existing in the liquid of radius R_o , with $\dot{R}_o = 0$, is dynamically stable.

However, these bubbles also slowly dissolve through diffusion of air out of the bubble. Evidence for the existence of these bubbles can be found in observing water as it is slowly heated. Near the temperature of 80°C , where the vapor pressure p_v is still less than the atmospheric pressure p_∞ , corresponding to the condition $\delta p < 0$, these bubbles can be seen floating within the body of the liquid or clinging to the container walls. Their duration although limited by diffusion is still long enough for visual observation.

A convenient way to plot $f(R)$ as a function of R for various initial values of p_{A_o} is to express p_{A_o} as some multiple of δp such as $p_{A_o} = \alpha \delta p$ and then change $f(R)$ to dimensionless form by dividing through by $\delta p + p_{A_o}$. Thus

$$\frac{f(R)}{\delta p + p_{A_0}} = \frac{\delta p}{\delta p + p_{A_0}} + \frac{p_{A_0}}{\delta p + p_{A_0}} \frac{R_0^3}{R^3} - \frac{2\sigma}{(\delta p + p_{A_0})R}$$

and with $u = \frac{R}{R_0}$, and

$$(1 + \alpha) \frac{f(R)}{\delta p + p_{A_0}} = f(u)$$

one gets

$$f(u) = 1 - \frac{1 + \alpha}{u} + \frac{\alpha}{u^3} \quad (10)$$

Figure 1 shows $f(u)$ as a function of u for various values of α .

The case $\alpha = 0$ corresponds to the growth of a vapor bubble.

The preceding analysis has shown that for the growth of a bubble as governed by the equation of motion

$$R \ddot{R} + \frac{3}{2} \dot{R}^2 = \frac{\delta p + p_{A_0} \frac{R_0^3}{R^3} - \frac{2\sigma}{R}}{\rho} \quad (11)$$

with initial conditions R_0 and \dot{R}_0 , the range of equilibrium bubble radii which are dynamically unstable is

$$\frac{4\sigma}{3\delta p} \leq R_0 \leq \frac{2\sigma}{\delta p}$$

where

$$\frac{\delta p}{2} \geq p_{A_0} \geq 0.$$

The solution of Eq. (11) is completed as follows: multiplying by $R^2 \dot{R}$ Eq. (11) becomes

or integrating from R_0 to R , one obtains

$$\begin{aligned} \dot{R}^2 = \frac{2}{3} \frac{\delta p}{\rho} - \frac{2\sigma}{\rho R} + 2 \frac{p_{A_0}}{\rho} \frac{R_0^3}{R^3} \log_e R \\ + \frac{R_0^3 \dot{R}_0^2 + \frac{2\sigma}{\rho} R_0^2 - \frac{2}{3} \frac{\delta p}{\rho} R_0^3 - 2 \frac{p_{A_0}}{\rho} R_0^3 \log_e R_0}{R^3} \end{aligned} \quad (12)$$

Thus

$$\dot{R}^2 \sim \frac{2}{3} \frac{\delta p}{\rho}, \quad R \rightarrow \infty.$$

This means that the bubble radius approaches a linear increase with respect to time as $R \rightarrow \infty$ or

$$R \sim \sqrt{\frac{2}{3} \frac{\delta p}{\rho}} t, \quad R \rightarrow \infty.$$

From Eq. (12) it is evident that the terms in $\frac{\log_e R}{R^3}$ and $\frac{1}{R^3}$ become small quite rapidly. Physically, this means that the effect of air in a bubble can be important to initiate the growth of the bubble, but its effect upon the subsequent behavior of the bubble radius is negligible; furthermore, all of the initial conditions such as R_0 and \dot{R}_0 are involved in the $\frac{1}{R^3}$ term which also vanishes quite rapidly as $R \rightarrow \infty$.

The solution of interest in this paper is the case where $p_{A_0} = 0$ which means that the equation of motion together with the initial conditions defines the rate of growth of a vapor bubble. Thus Eq. (11) becomes

$$R\ddot{R} + \frac{3}{2} \dot{R}^2 = \frac{\delta p - \frac{2\sigma}{R}}{\rho}. \quad (13)$$

Setting the right hand side equal to zero, one obtains the equilibrium radius

which together with the condition $\dot{R}]_{R=R_0} = 0$ defines the initial equilibrium size of the vapor bubble. Figure 2 shows a plot of δp as a function of the temperature T , taking the value of $P_{\infty} = 1$ normal atmosphere. Figure 3 is a plot of R_0 as a function of the temperature T , with the values for σ corresponding to appropriate values of T . It is convenient to express Eq. (13) in dimensionless form. This can be done by letting

$$u = \frac{R}{R_0}, \quad \chi = \frac{t}{R_0} \sqrt{\frac{\delta p}{\rho}}, \quad \dot{u} = \frac{d u}{d \chi}.$$

Equation (13) then becomes

$$u \ddot{u} + \frac{3}{2} \dot{u}^2 = 1 - \frac{1}{u} \quad (14)$$

Multiplying Eq. (14) by $u^2 \dot{u}$ and integrating from u_i to u , where u_i is the dimensionless radius at some initial time of χ_i one gets

$$\dot{u}^2 = \frac{2}{3} - \frac{1}{u} + \frac{u_i^3 \dot{u}_i^2 - \frac{2}{3} u_i^3 + u_i^2}{u^3} \quad (15)$$

where \dot{u}_i is the velocity of the bubble wall for $\chi = \chi_i$. Let $C = u_i^3 \dot{u}_i^2 - \frac{2}{3} u_i^3 + u_i^2$, where C is a constant taking on various values depending upon the values chosen for u_i and \dot{u}_i . Figure 4 shows a plot of

$$\dot{u} = \pm \sqrt{\frac{2}{3} - \frac{1}{u} + \frac{C}{u^3}} \quad (16)$$

for various values of C . The significance of the graph is as follows: by choosing a point (u, \dot{u}) on the graph as an initial value determines the value of C and hence prescribes the subsequent behavior of the bubble radius as governed by Eq. (16). Thus picking a value of $u_i < 1$ and $\dot{u}_i = 0$ means that the bubble will collapse, or picking a value of $u_i > 1$ and $\dot{u}_i = 0$ means that the bubble will grow. The point $u_i = 1, \dot{u}_i = 0$ is a singular point since a bubble in this state remains in equilibrium, or loosely speaking, it takes an infinite time for the bubble to increase or decrease in size. However, this equilibrium is dynamically unstable. In the actual physical case such an equilibrium would soon be upset by a slight change in temperature. Taking the positive root of Eq. (16) and integrating one gets

$$\gamma - \gamma_i = \int_{u_i}^u \frac{dx}{\sqrt{\frac{2}{3} - \frac{1}{x} + \frac{C}{x^3}}}$$

or with the change in variable $y = \frac{1}{x}$, the integral becomes

$$\gamma - \gamma_i = \int_{\frac{1}{u}}^{\frac{1}{u_i}} \frac{dy}{y^2 \sqrt{\frac{2}{3} - y + Cy^3}} \quad (17)$$

The integral in Eq. (17) is an elliptic integral except when $C = \frac{1}{3}$ and 0.

For the case $C = \frac{1}{3}$ Eq. (17) can be expressed as

$$\gamma - \gamma_j = \sqrt{3} \int_{\frac{1}{u}}^{\frac{1}{u_j}} \frac{dy}{y^2 (y-1) \sqrt{y+2}} \quad (18)$$

This corresponds to the case $u_i = 1$, $\dot{u}_i = 0$ in the expression for C. The limit here, must be $\frac{1}{u_j} < \frac{1}{u_i}$ and $\chi_j > \chi_i$ since a limit of $\frac{1}{u_i} = 1$ means that the integral becomes infinite or the bubble does not grow. By choosing a value $u_j > 1$ automatically starts the bubble along the trajectory for $C = \frac{1}{3}$ at some value u_j and $\dot{u}_j \neq 0$. The closer one picks u_j to 1, the longer it will take the bubble to grow. The integration of Eq. (18) is readily carried out by a separation of the integrand into partial fractions resulting in the following relation between χ and u :

$$\begin{aligned} \chi - \chi_j = & \frac{u}{2} \sqrt{\frac{3}{u} + 6} - \frac{u_j}{2} \sqrt{\frac{3}{u_j} + 6} \\ & + \frac{3}{4} \sqrt{\frac{3}{2}} \log_e \left\{ \frac{\frac{u}{2} \sqrt{\frac{3}{u} + 6} + \sqrt{\frac{3}{2}} (u + \frac{1}{4})}{\frac{u_j}{2} \sqrt{\frac{3}{u_j} + 6} + \sqrt{\frac{3}{2}} (u_j + \frac{1}{4})} \right\} \\ & - \log_e \left[\left(\frac{u_j - 1}{u - 1} \right) \left\{ \frac{\frac{u}{2} \sqrt{\frac{3}{u} + 6} + \frac{5}{4} (u + \frac{1}{5})}{\frac{u_j}{2} \sqrt{\frac{3}{u_j} + 6} + \frac{5}{4} (u_j + \frac{1}{5})} \right\} \right]. \end{aligned} \quad (19)$$

Figure 5 is a plot of χ as a function of u as expressed by Eq. (19) for $u_j = 1.01$ and $u_j = 1.000001$ and shows the effect of taking u_j close to $u_i = 1$. Figures 6a and 6b are plots of the actual radius R , as a function of the time t , for various liquid temperatures using Eq. (19).

The assumption has been made that the vapor pressure has a constant value throughout the growth of the bubble. However, evaporation is a process which proceeds at a finite rate and if this

rate is not sufficiently high to keep up with the rate of volume change in the bubble, the vapor in the bubble will behave more like a permanent gas. Plesset tested this assumption for the case of a cavitation bubble⁽¹⁾ with an estimate of evaporation rates based on kinetic theory. A similar analysis can be applied here. Thus the rate of evaporation is estimated from kinetic theory which says that the mass of gas evaporated per unit area per unit time at an absolute temperature T, for water is

$$j = .04 p_v \sqrt{\frac{M}{2\pi B T}} \quad , \quad (20)$$

where p_v denotes the vapor pressure for a vapor with molar mass M, and B is the gas constant. If one assumes that the vapor obeys the perfect gas law

$$p_v = \frac{e'}{M} B T \quad ,$$

which is reasonably accurate in the temperature range of interest⁽⁷⁾,

Eq. (20) may be written

$$j = .04 e' \sqrt{\frac{B T}{2\pi M}} = e' V$$

where $V = .04 \sqrt{\frac{B T}{2\pi M}}$ is the desired velocity to be associated

with the rate of the evaporation process. For the present problem,

at 105°C, V is approximately 670 cm. per sec. This compared to

$\dot{R} \Big|_{R \rightarrow \infty} = 356$ cm. per sec. for the bubble growth at 105°C is seen to be

quite large. Thus the assumption of p_v constant, as far as evaporation rates are concerned, is reasonable.

3. Plesset-Zwick Theory for Bubble Growth

The problem up to this point has been to assume that the bubble expands isothermally, that is, the vapor pressure has been assumed to remain constant throughout the expansion process, having a value corresponding to the bulk temperature of the water. Now this assumption is nearly correct if one thinks of this in terms of the actual variation in the vapor pressure as compared to the absolute initial value of the vapor pressure. However, in terms of the mechanism of bubble growth the variation in vapor pressure has a marked effect on the rate of growth. Heat must be applied to the bubble to evaporate water and maintain the vapor pressure during growth. The total mass of vapor which is evaporated into the bubble for a radius R , is $\frac{4}{3} \pi R^3 \rho'$ where ρ' is the vapor density. The total heat required is $Q = \frac{4}{3} \pi R^3 \rho' L$ where L is the latent heat of evaporation. This heat is taken out of a water layer surrounding the bubble. If the thermal diffusivity of water is D and the time required to grow to a radius R is t , then the order of magnitude of the layer is $\delta \approx \sqrt{Dt}$. Thus the problem as formulated by Plesset and Zwick⁽⁸⁾ is to first consider the problem of non-steady heat diffusion which is encountered in dealing with the dynamics of a vapor bubble in a heated liquid. From this problem one obtains the variation of the temperature at the bubble wall as a function of time.

The heat conduction problem is formulated as follows: the liquid is assumed to be non-viscous and incompressible, and the thermal

conductivity k , density ρ , and specific heat C , of the liquid are assumed to have insignificant variation with temperature. The temperature T in the liquid then satisfies the equation

$$\Delta T = \frac{1}{D} \frac{dT}{dt} - \frac{1}{k} \dot{\eta} \quad (21)$$

Here $D = \frac{k}{\rho C}$ is the thermal diffusivity of the liquid, $\eta = \eta(t)$ is the heat source per unit volume in the liquid which is taken to be a function of time only, and $\frac{dT}{dt}$ denotes the particle derivative so that

$$\frac{dT}{dt} = \frac{\partial T}{\partial t} + \bar{V} \cdot \nabla T,$$

where \bar{V} is the liquid velocity which in general varies with position and time. It is assumed that the motion possesses spherical symmetry; i.e., the vapor bubble is spherical, and its radial motion is sufficiently rapid that any translational motion may be neglected. The Eulerian coordinates are chosen as (r, t) with $r = 0$ at the center of the bubble. $R = R(t)$ is the bubble radius at time t . The temperature at $r = \infty$ is T_0 for time $t = 0$, or the temperature for a later time t , at infinity is $T_\infty = T_0 + \frac{D}{k} \eta(t)$, where $\eta(0) = 0$, and the temperature at $t = 0$ is T_0 everywhere. This diffusion problem is then solved assuming that the thermal boundary layer is very thin compared to the bubble radius. For the case of the vapor bubble in a liquid, this assumption is made plausible by the fact that not only is the heat capacity much greater in the liquid state than in the vapor state but the thermal diffusivity is about

1000 times smaller. Thus the zeroth order approximation for the difference between the temperature at the spherical boundary, $T(0, t)$ and the initial temperature of the liquid T_0 is given by

$$T(0, t) - T_0 = \frac{D}{K} \eta(t) - \left(\frac{D}{\pi}\right)^{\frac{1}{2}} \int_0^t \frac{R^2(x) \left(\frac{\partial T}{\partial r}\right)_{r=R(x)}}{\left\{ \int_x^t R^4(y) dy \right\}^{\frac{1}{2}}} dx. \quad (22)$$

Now the mass of vapor in the bubble is given by

$$m = \frac{4}{3} \pi R^3(t) \rho'$$

or with L = latent heat of evaporation, the heat content is $Q = Lm$; therefore

$$\frac{dQ}{dt} = L \frac{dm}{dt} = \frac{4}{3} \pi L \frac{d}{dt} \left\{ R^3(t) \rho' \right\},$$

but this is also equal to

$$4 \pi R^3(t) K \left(\frac{\partial T}{\partial r} \right)_{r=R(t)}$$

so that

$$\left(\frac{\partial T}{\partial r} \right)_{r=R(t)} = \frac{L}{3 K R^3(t)} \frac{d}{dt} \left\{ R^3(t) \rho' \right\}.$$

For small temperature variations, ρ' is nearly constant, giving

$$\left(\frac{\partial T}{\partial r} \right)_{r=R(t)} = \frac{L \rho' \dot{R}(t)}{K} = \frac{L}{DC} \frac{\rho'}{\rho} \dot{R}(t).$$

Thus Eq. (22) can be written as

$$T(o, t) - T_o = \frac{D}{k} \eta(t) - \frac{L}{c\sqrt{\pi D}} \frac{\rho'}{\rho} \int_0^t \frac{R^2(x) \dot{R}(x)}{\left\{ \int_x^t R^2(y) dy \right\}^{\frac{1}{2}}} dx.$$

For the present problem the vapor pressure can be expressed as

$$p_v(T) = p_v(T_o) + A \{T(o, t) - T_o\} + B \{T(o, t) - T_o\}^2.$$

Thus the equation of motion becomes

$$R \ddot{R} + \frac{3}{2} \dot{R}^2 = \frac{p_v(t) - p_\infty - \frac{2\sigma}{R}}{\rho}.$$

This problem⁽⁹⁾ is then solved to find the rate of growth of the vapor bubble. The mechanism for growth from the equilibrium size $R_o = \frac{2\sigma}{p_v(o) - p_\infty}$ is provided by giving $\eta(t)$ a very small increase starting at $t = 0$. This increase becomes insignificant as the growth progresses and is a mathematical means for getting the bubble started just as in the case of the solution with p_v constant, a slightly larger initial radius than $R_o = \frac{2\sigma}{p_v - p_\infty}$ was chosen to get the bubble started.

It has been assumed here that the temperature of all the vapor in the bubble has the same value as the bubble wall temperature throughout the entire volume of vapor. This is made plausible by the fact that the thermal diffusivity D , for the water vapor is 1000 times as great as that for water.

A plot of the radius R , as a function of the time t , is shown in Figure 14 for a temperature of 103.05°C for the Plesset-Zwicky

Theory and is compared to the solution obtained with the extended Rayleigh Theory for the same temperature. The marked effect that the cooling of the bubble wall has on reducing the rate of growth is apparent. Thus the Rayleigh Theory predicts that the bubble approaches a linear rate of growth as the radius increases, the rate being $\dot{R} = \sqrt{\frac{2}{3} \frac{\delta p}{\rho}}$, whereas the Plesset-Zwicky Theory predicts that as the bubble grows the cooling of the bubble wall due to evaporation of the vapor results in the vapor pressure p_v , approaching the value of the atmospheric pressure p_∞ , or $\delta p \rightarrow 0$ as $R \rightarrow \infty$; hence $\dot{R} \rightarrow 0$. Consequently a cooling of, say, 2°C may be small compared to 102°C , but in terms of the 2°C of superheat corresponding to the value of δp , this cooling results in $\delta p \rightarrow 0$. Since the driving force for the bubble growth is produced by δp , its variation has a pronounced effect upon the rate of growth.

III. APPARATUS AND PROCEDURE

1. Heating the Water

The requirements for obtaining vapor bubble formation within the body of the liquid at various degrees of superheat are apparent in theory, but the actual realization of such a condition requires a variation in the usual means for boiling water. The requirements are that the liquid must be heated slowly and uniformly, and the walls of the container of the liquid must not be subjected to temperatures so great that a very large thermal gradient exists within a very narrow boundary adjacent to the walls. In addition, these surfaces must be clean and free of pits or scratches. In the case of such gradients all of the bubbles form either within this layer or actually form on the solid surfaces of the container. Thus in the case of heating a beaker of water with a bunsen burner most of the bubbles form at the bottom of the beaker and quickly rise out of the thermal layer and intermix with the main body of the liquid. In this way one has a condition closely approximating the dynamic equilibrium of many large bubbles in the body of the liquid. This condition is realized by the fact that as the bubbles grow they rise into the cooler regions of the liquid above the thermal boundary layer, and their rates of growth are decreased to a point where the bubble can be assumed to be in dynamic equilibrium with the liquid. Since these bubbles are very large, the effects of surface tension are negligible; hence the

vapor pressure inside the bubble is very nearly equal to the external pressure on the liquid, which for water heated in a beaker in the laboratory is essentially the atmospheric pressure. Thus the temperature of the boiling water will be very close to that corresponding to the vapor pressure being equal to the atmospheric pressure. For the case of one normal atmosphere of pressure, this temperature will be 100°C .

In order to heat the water uniformly the following procedure was used: a beaker was constructed from pyrex tube stock $2\frac{1}{2}$ in. diameter. The tube was cut into a 6 in. length and a beaker was formed from the tube with a flat face $1\frac{1}{4}$ in. wide and 6 in. high. This was done for photographic purposes. The beaker was annealed very carefully to make the inner surface very smooth and free from pits. The beaker was cleaned before each experiment with a detergent to remove any oil films present on the surface of the beaker. The water used in the tests was doubly distilled, and for some of the tests was contaminated with solid impurities such as powdered chalk or sand to produce various degrees of superheat. The water was first boiled in a large container for about one hour to remove most of the air in the water. Water boiled in this way contains about 20% of the initial air content. This was not done in the beaker since too much water would evaporate from the test sample. The container with water thus treated was heated by two 250 Watt reflector-type

infra-red lamps with the beaker located between the lamps.

Figure 7 shows the setup of lamps and beaker. In this way 300 cc. of water can be brought to the boiling point in about 10 minutes. Attempts at obtaining vapor bubbles in the body of the liquid with this technique were completely successful and yielded superheat temperatures up to 107°C .

The reasons for the success of this method can best be obtained by considering the nature of the radiation of the infra-red lamps and the absorption of this radiation by the beaker and the water. The infra-red lamp is rated at 250 watts for a line voltage of 115 volts. Under these conditions the tungsten filament temperature is 2500°K . Since the lamp radiates nearly as a black body, according to factory specifications, Wien's displacement law can be used to obtain the wave length corresponding to the maximum energy output. Thus for 2500°K , $\lambda_{max} = 1.16 \mu$ ($\mu = 10^{-4} \text{ cm.}$). The distribution corresponding to this temperature shows that approximately 3% of the radiant energy lies between, $.4 \mu$ to $.7 \mu$ (visible light region). Since the tungsten filament is enclosed by a pyrex bulb, a certain amount of the radiation is absorbed by the bulb itself. Now pyrex is essentially transparent to radiation from $.3 \mu$ to 3μ , but beyond 3μ a sheet of pyrex 2 mm. thick absorbs nearly all the radiation. This accounts for about 17% of the total radiated energy originating from the tungsten filament. Thus approximately

80% of the total radiated power is available for heating over a wave band from $.7\mu$ to 3μ . Since the beaker itself is pyrex about 2 mm. thick, it will transmit most of the radiation transmitted by the bulb itself. Thus one attains the desired effect of not having the beaker at higher temperatures than the main body of water. The water itself is an excellent absorber of infra-red radiation especially from $.97\mu$ up to 3μ which is 68% of the total radiated energy. ⁽¹⁰⁾ For example, a layer of water 1 cm. thick absorbs 38% of the radiation of $\lambda = 1\mu$ and 95% of that at $\lambda = 1.4\mu$ and essentially all the radiation is absorbed in this layer for values of $\lambda > 1.4\mu$. The remaining 12% of the total radiation from $.7\mu$ to $.97\mu$ is also absorbed but to a lesser extent. The fact that the water is heated very slowly means that the slight thermal gradients existing in the liquid are removed by heat conduction. Thus the temperature of the liquid is raised essentially in a uniform fashion. This is born out by temperature measurements throughout the bulk of the liquid.

2. Temperature Measurements

The selection of the temperature measuring device was controlled primarily by the necessity for having an instrument which could be placed in the water without having bubbles form from the device, since this would eliminate the possibility of having the bubbles form in the body of the liquid. With this restriction, a mercury-in-glass

thermometer was chosen since the bulbs of most thermometers have a very smooth surface as a result of annealing, and hence provide, in most cases, a surface even more favorable to the prevention of bubble formation than the beaker itself. The thermal lag of the thermometer was not an important factor for these experiments since the only runs considered were those for which the temperature remained nearly constant within $.1^{\circ}\text{C}$ during a given test the duration of which exceeded the time of any thermal lag by a wide margin. The actual thermometer used in the experiments was a Braun Nitrogen-filled mercury-in-glass thermometer with a range of 100°C - 200°C graduated in $.1^{\circ}\text{C}$. The thermometer was immersed up to a point just short of the graduations to avoid bubbling from the etched portions of the stem. This meant that the mercury column extended out of the water for all temperatures above 100°C , and thus a correction to the temperature reading would be necessary. Using the correction formula from the Bureau of Standards⁽¹¹⁾ the maximum correction found necessary was approximately $.005^{\circ}\text{C}$. Since this is negligible in terms of $.1^{\circ}\text{C}$ accuracy, this correction was neglected. Another factor affecting the true temperature reading was the fact that the thermometer was not shielded from the effects of radiation. In the discussion on heating water it was shown that the band of infra-red radiation from $.7\mu$ to $.97\mu$ is the least absorbed by the water, and hence this portion of the radiant energy (12% of the total) is incident upon the thermometer. It should be pointed out that the thermometer was

at all times about 2 cm. from the walls of the beaker. Thus a layer of 2 cm. of water was available for the actual absorption of the radiant energy. The bulb of the thermometer is essentially transparent to the range of radiation from $.7\mu$ to $.97\mu$ and the mercury in the bulb is a good reflector of radiation and absorbs very little radiation. Thus it could be said that the water acts as a radiation shield for the thermometer, and the radiation effect on the true temperature reading is negligible in terms of the accuracies in the present measurements. To test this, a shield was made of aluminum tubing for the thermometer. The temperature reading for a thermometer without the shield was compared with the reading of the shielded thermometer and the result was that the two simultaneous readings never varied more than $.1^{\circ}\text{C}$. The temperature variation throughout the bulk of the liquid was checked after the water had reached a state of boiling, and the variations were found to be much smaller than $.1^{\circ}\text{C}$. The accuracy of this type of thermometer is within $\pm .1^{\circ}\text{C}$. Thus considering the two largest errors, namely, the accuracy of the thermometer and the variation in the temperature during a test, the temperature readings obtained are assumed accurate within $.2^{\circ}\text{C}$.

3. Photographic Procedure

The photographic equipment used in this study was of the multi-flash type. It consisted of a simple camera in which the recording film moves constantly past the focal plane at a high speed.

The camera has no shutter, hence the illumination which was provided by a flash lamp also acted as the shutter. This required that the flash duration be so short that neither the image of the object on the film nor the film itself move an appreciable distance while the light was on. For the present experiments pictures were taken at a rate of 1000 exposures per second. This rate was found fast enough to record the growth of a vapor bubble and still give a normal sized 35 mm. picture. The camera itself was the standard General Radio type of instrument as shown in Figure 7 fitted with an f 1.5 Kodak Ektar 2" lens. The film used was Eastman 35 mm. Back-ground X and was run through the camera at an average rate of 100 feet per second. The flash lamps used were of the type originally developed by Professor Harold E. Edgerton and his associates at M.I.T. A detailed account is given in Reference 12.

Since there is no practical way of knowing just where or when a bubble will form, the chances of catching a bubble on a strip of film 50 ft. long which runs through the camera in about $\frac{1}{2}$ sec. is very small and depends on the area of view and the depth of focus. Thus the choice of magnification depends upon the following factors: it is desirable to have great magnifications since the detail in the pictures of small bubbles will be clearer. However a factor of two in the picture size of the radius of the bubble diminishes the area of view by a factor of four and reduces the depth of focus. It was found that magnifications from .5X to 4X were practical in the

sense of the amount of film used and the time involved to obtain a bubble history. This difficulty was coupled with the fact, that, if during a run the temperature variation was too great, even a successful bubble history from the photographic view point was useless in terms of useable data for the rate of growth. The overall efficiency of this method was to obtain a useable bubble history per 150 feet of film.

With a magnification of 1X the depth of focus was about $\frac{1}{8}$ in. The magnification was determined by placing a scale in the water and focusing on a piece of film in the camera. Thus any bubble in focus could be assumed to have the appropriate magnification corresponding to the setting of the camera since the depth of focus was so small. All of the bubble diameters were measured directly from the negative with a microscopic comparitor. Each bubble was measured three times and the average value was taken. The actual measurements of the bubble diameters are estimated to be correct within 3% using this technique.

IV. ANALYSIS OF DATA AND THEORY

1. Analysis of the Data

Since the bubbles rise through the liquid as they grow, they cannot be called spherical bubbles in the strict sense of the word. As the bubbles rise they tend to assume a shape similar to an oblate spheroid. This effect is very slight during the first part of the growth because the translational motion is very slow compared to the rate of growth of the bubble. During the latter part of the growth the translational effect is very great compared to the rate of growth, and essentially determines the shape of the bubble. As an approximation, the translational motion of the bubble can be compared to the translational motion of a rigid sphere in a fluid. The pressure distribution along the boundary of the sphere⁽¹³⁾ is given by

$$p = \frac{1}{2} \rho U^2 \left(1 - \frac{9}{4} \sin^2 \theta \right) + p_{\infty} \quad (23)$$

where U is the velocity of the sphere, p_{∞} is the static pressure at infinity, and θ is measured from the axis in the direction of motion. From Eq. (23) it can be seen that the pressure at the nose and aft end of the sphere are at a maximum, and the pressure gradually diminishes to a minimum at the sides. Thus for the case of a bubble the net result is that the dimension of the bubble is reduced in the direction of motion and increased at right angles to the motion.

However the bubble dimensions measured from the negatives were restricted to bubbles occurring during the first part of the growth. Thus the diameter measured in the horizontal plane does not exceed the diameter in the vertical plane by more than 3% (the horizontal measurement was used for the data). The effect of translation on the conduction of heat is caused by the fact that as the bubble rises, it enters a hotter region than it would normally experience if it grew without any translational motion and extracted heat from the same region. Hence the rate of growth should be somewhat higher in the actual case than in the Plesset-Zwicky theory where the assumption is made that there is no translational motion of the bubble. However, the amount of translation in the bubble histories is less than twice the diameter of the first bubble measured. This can be seen from Figure 8 which shows an actual bubble history. Thus this effect, although present, is very small.

The effects of the walls of the container and the proximity of other bubbles were neglected since these distances were large compared to the bubble sizes considered and thus their effects on the bubble growth are probably less than the uncertainty of the data.

Since the time between each picture is .001 second, there is an uncertainty in the exact time when the bubble starts to grow from the dynamic equilibrium radius. Thus this time lies between the first visible bubble picture and the frame showing no bubble. Hence one

is free to shift the time axis for any bubble history up to the amount of .001 second. This allows one, when comparing bubble histories at a given temperature, to shift the point on the graph \pm .001 sec. in time to obtain the best fit. In a sense this uncertainty helps in making the comparisons of several bubble histories seem better than they may actually be. However this does not alter the actual slopes of the radius-time curves.

Since the temperature measurements are estimated to be accurate within $.2^{\circ}\text{C}$, the corresponding accuracy of the vapor pressure is required. As an example, the thermal rate of variation of the vapor pressure for the temperature range of 100°C to 105°C is approximately $4 \times 10^4 \frac{\text{dynes}}{\text{cm}^2 \text{ } ^{\circ}\text{C}}$ or for $.2^{\circ}\text{C}$ this gives an error of $8 \times 10^3 \frac{\text{dynes}}{\text{cm}^2}$. Now this error is very small when compared to vapor pressures of the order of $10^6 \frac{\text{dynes}}{\text{cm}^2}$ for the temperature range of interest. However in terms of $\delta p = p_v - p_{\infty}$, which is really the important factor for bubble growth, the order of magnitude is 10^5 . Therefore, the error in δp caused by an error of $.2^{\circ}\text{C}$ in the thermometer reading is approximately 8%. Since the bubble velocities are roughly proportional to $\sqrt{\frac{\delta p}{\rho}}$, the errors in the general slopes of the radius-time curves obtained from the data should be in error by about 4% from temperature errors alone. This error together with the errors in the negative measurements yields an estimated overall error in the bubble radii, of 10%.

Several bubble histories were obtained for five different temperatures. In some cases all the bubbles for a given temperature were obtained during one run, and for others the histories were obtained from independent runs. Thus Bubbles #1 and #3 are from one reel and Bubble #2 from another reel, Figure 9. Bubbles #5 and #6 are from one reel and Bubble #4 is from another reel, Figure 10. Bubbles #7, #8, and #9 are from separate reels, Figure 11. Bubbles #11 and #12 are from one reel and Bubble #10 is from another reel, Figure 12. Bubbles #13 and #14 are from the same reel, Figure 13. For Bubble #13 two points are missing because the film was blacked out for these two points.

2. Comparison of Data and Theory

The only calculation to date from the Plesset-Zwick theory is for the case $T = 103.05^{\circ}\text{C}$. Figure 14 shows a comparison between the extended Rayleigh Theory and the Plesset-Zwick Theory with Bubble #8. From the figure it can be seen that the effect of cooling of the bubble wall has a great effect on the rate of growth. The data follows the Plesset-Zwick Theory very closely as compared to the Rayleigh Theory. Thus the cooling of the bubble wall affects the dynamics of the bubble growth to a very marked extent. Hence the converse effect of condensation of vapor during the collapse of a vapor bubble may produce a lower rate of collapse than anticipated. This is so since the bubble wall will experience a temperature rise causing an increase in the vapor pressure.

REFERENCES

1. M. S. Plesset, Journal of Applied Mechanics, (1949), Vol. 71, pp. 277.
2. E. Newton Harvey, W. D. McElroy and A. H. Whitely, Journal of Applied Physics, (1947), Vol. 18, pp.162.
3. D. C. Pease and L. R. Blinks, Journal of Physical and Colloid Chemistry, (1947), Vol. 51, pp. 556.
4. J. Frenkel, Kinetic Theory of Liquids, Oxford University Press, (1946), pp. 372.
5. Lord Rayleigh, Philosophical Magazine, (1917), Vol. 34, pp.94-98.
6. M. S. Plesset and P. S. Epstein, Journal of Chemical Physics, (1950), Vol. 18, pp.1505.
7. N. E. Dorsey, Properties of Ordinary Water Substances, Reinhold Publishing Company, New York, N. Y., (1940), table 250, pp. 575-576.
8. M. S. Plesset and S. A. Zwick, Journal of Applied Physics, (1952), Vol. 23, pp.95.
9. M. S. Plesset and S. A. Zwick, Unpublished, California Institute of Technology, Pasadena, California.
10. N. E. Dorsey, Properties of Ordinary Water Substances, Reinhold Publishing Company, New York, N.Y., (1940), table 160, pp.326.
11. Johanna Busse, Temperature (Its Measurement and Control in Science and Industry), American Institute of Physics, Reinhold Publishing Company, New York, N. Y., (1941), p.237.
12. R. T. Knapp and A. Hollander, Trans. of the ASME, (1948), Vol. 70, p. 420.
13. L. M. Milne-Thompson, Theoretical Hydrodynamics, The Macmillan Company, New York, N. Y., (1950), p. 413.

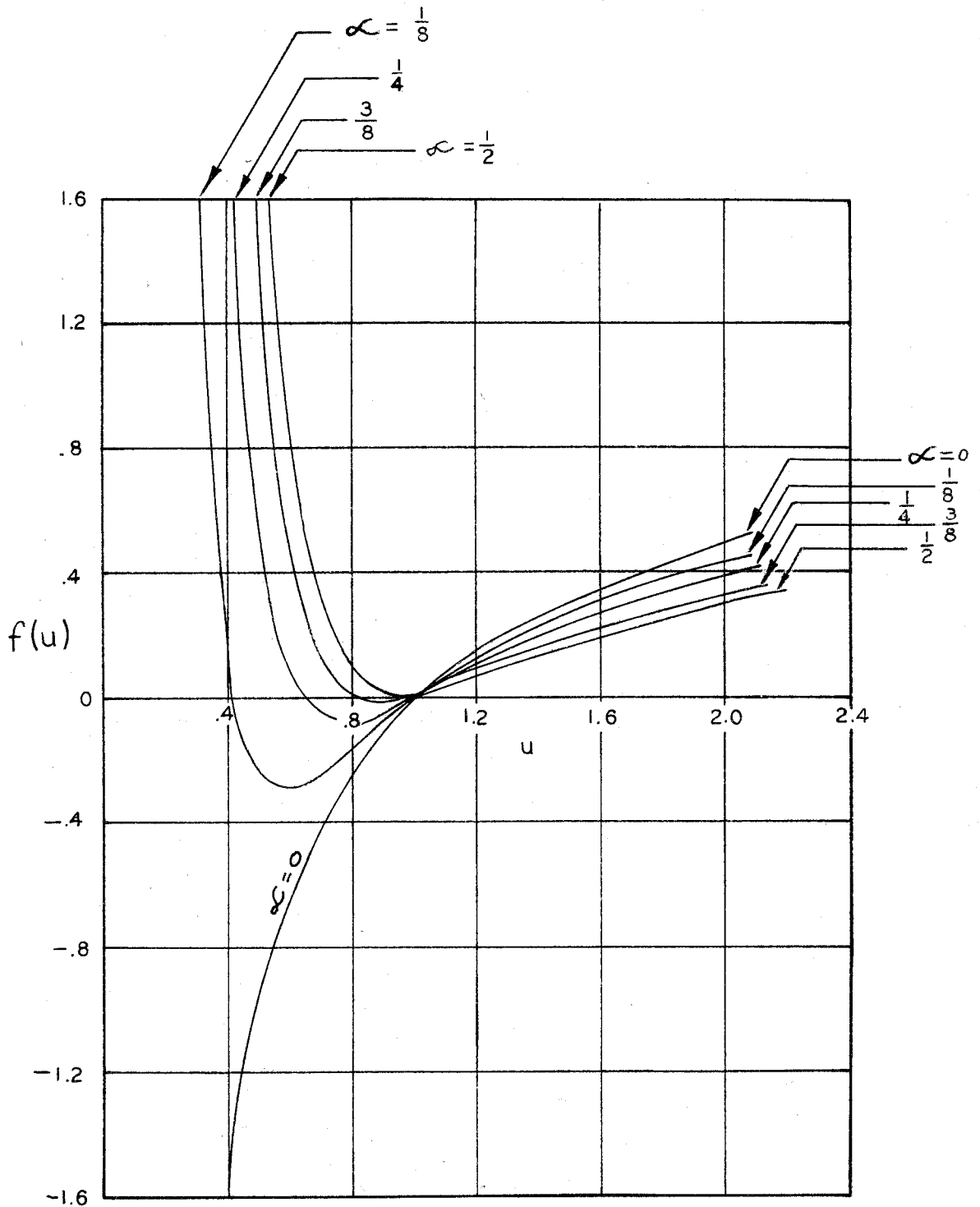


Fig. 1 - The function $f(u)$, which is the dimensionless form for the total pressure $f(R)$ acting on the bubble wall, is shown as a function of u as expressed by Eq. (10). The case $\alpha = 0$ corresponds to a vapor bubble.

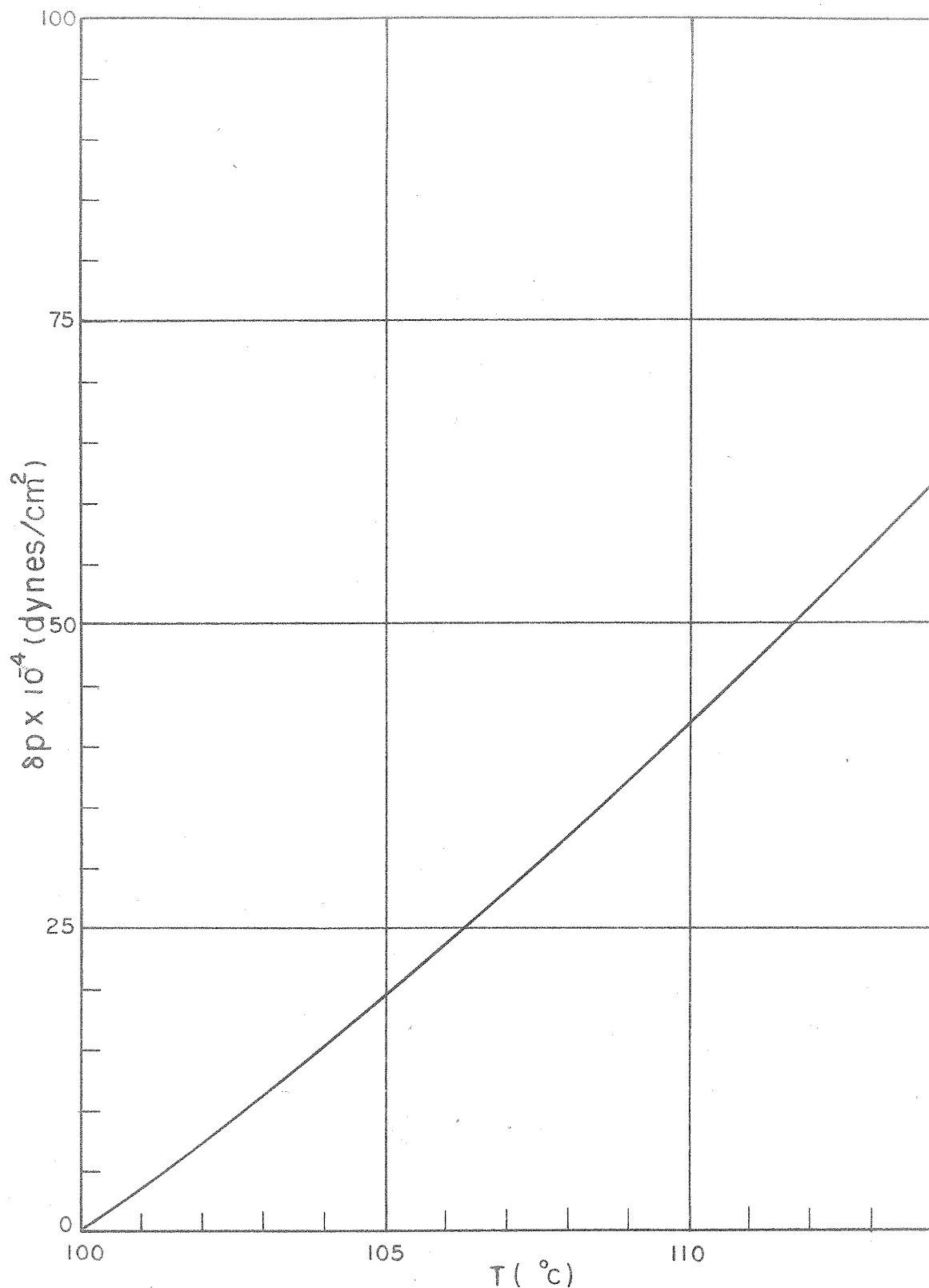


Fig. 2 - The difference between the vapor pressure and the atmospheric pressure, δp , is shown as a function of the water temperature, T . The value for the atmospheric pressure, p_{∞} is taken as $1.01325 \times 10^6 \text{ dynes/cm}^2$.

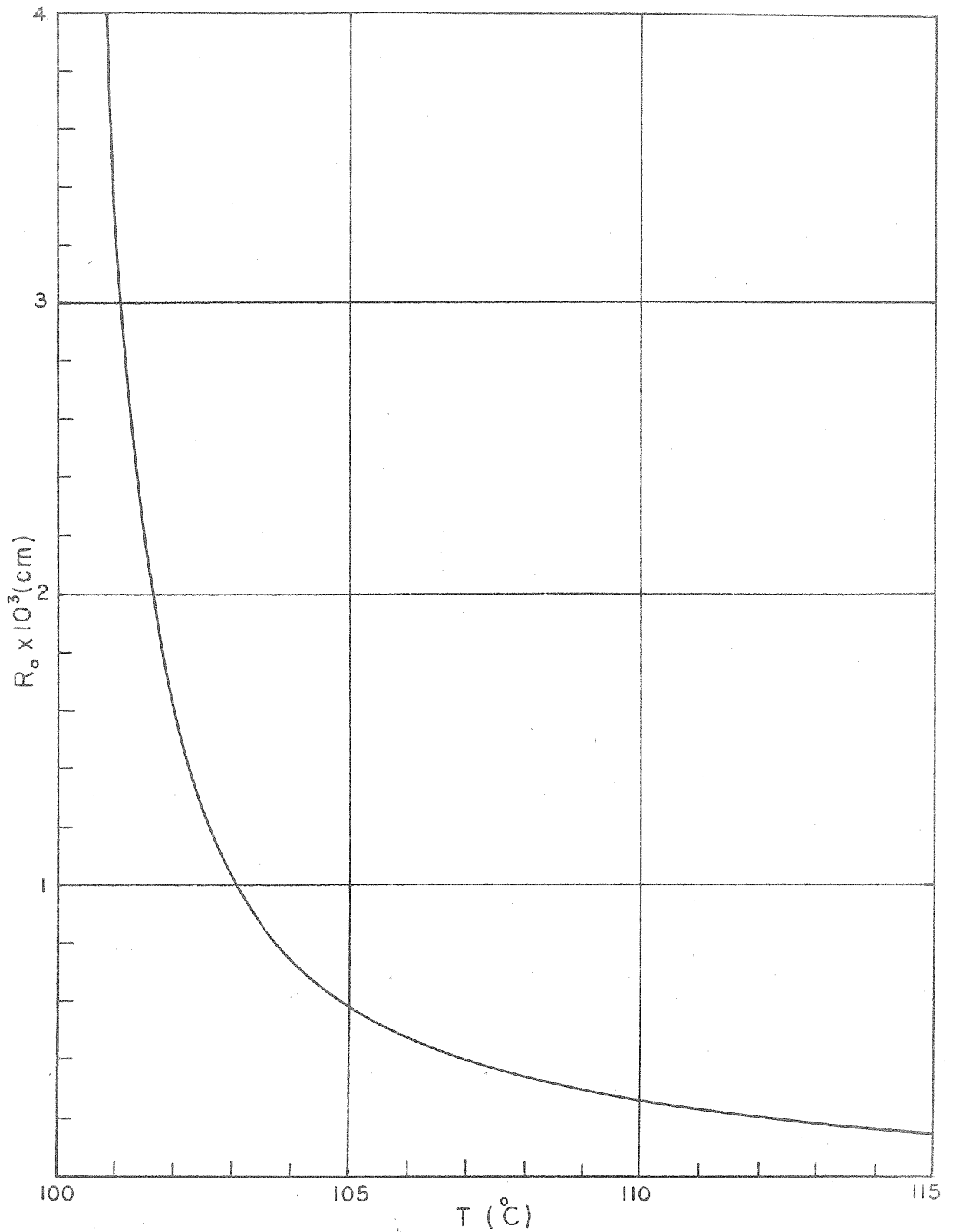


Fig. 3 - The radius $R_o = 2\sigma/\delta p$, for the dynamic equilibrium of a vapor bubble is shown as a function of the water temperature, T .

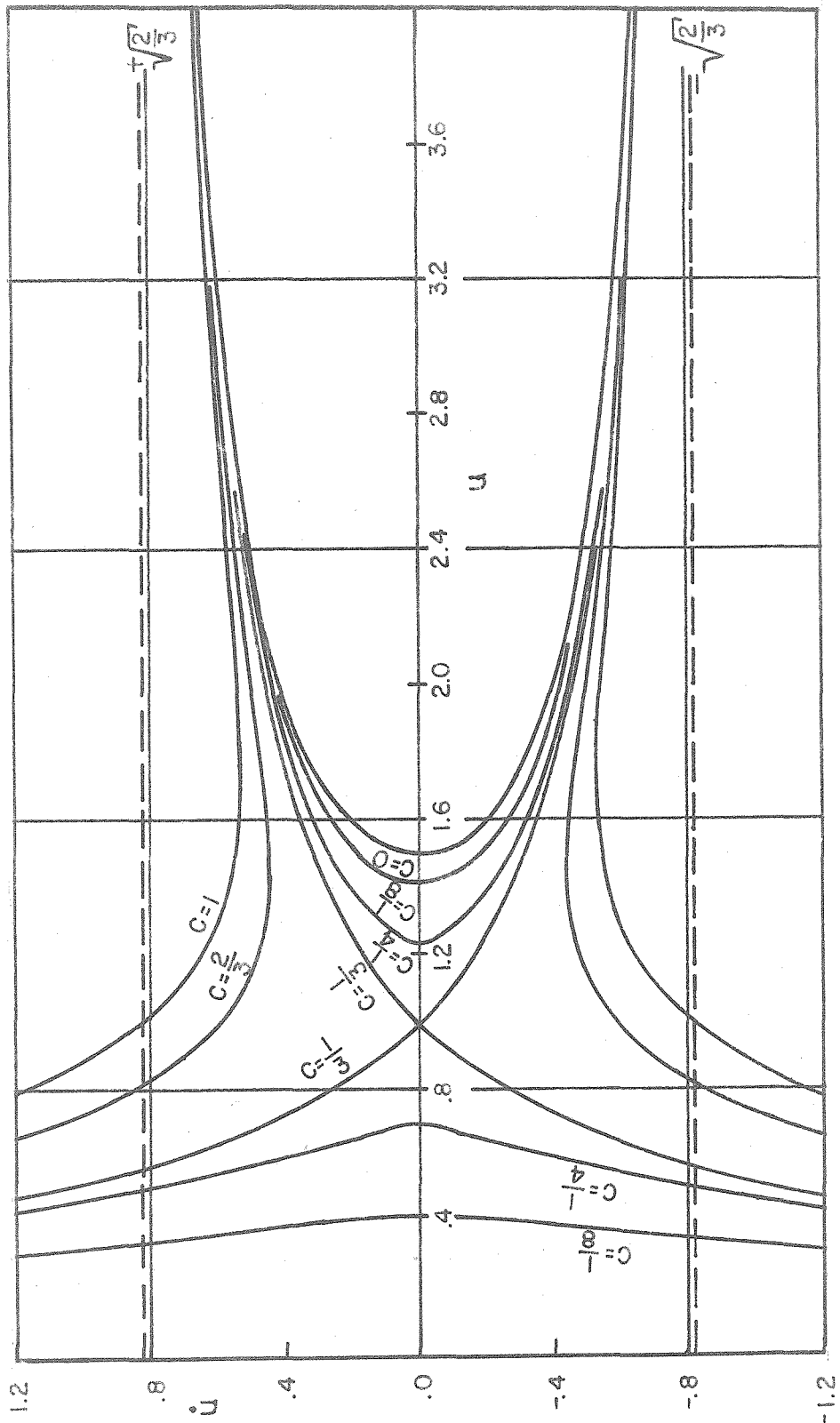


Fig. 4 - The dimensionless velocity u for various values of c is shown as a function of the dimensionless radius u as expressed by Eq. (16).

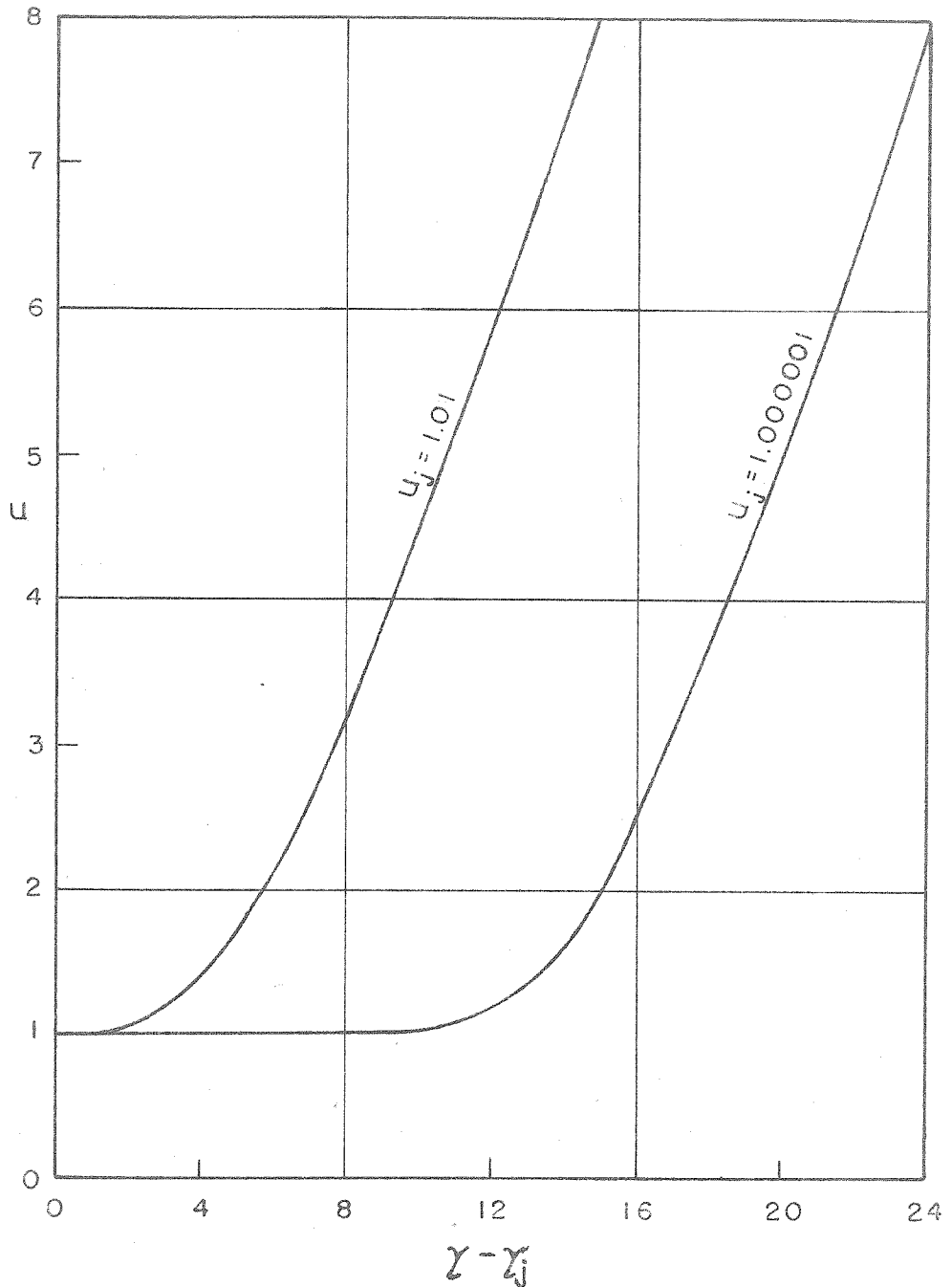


Fig. 5 - The dimensionless bubble radius u is shown for two initial values of the bubble radius u_i corresponding to the time τ_i as a function of the dimensionless time $\tau - \tau_i$, as expressed by Eq. (19).

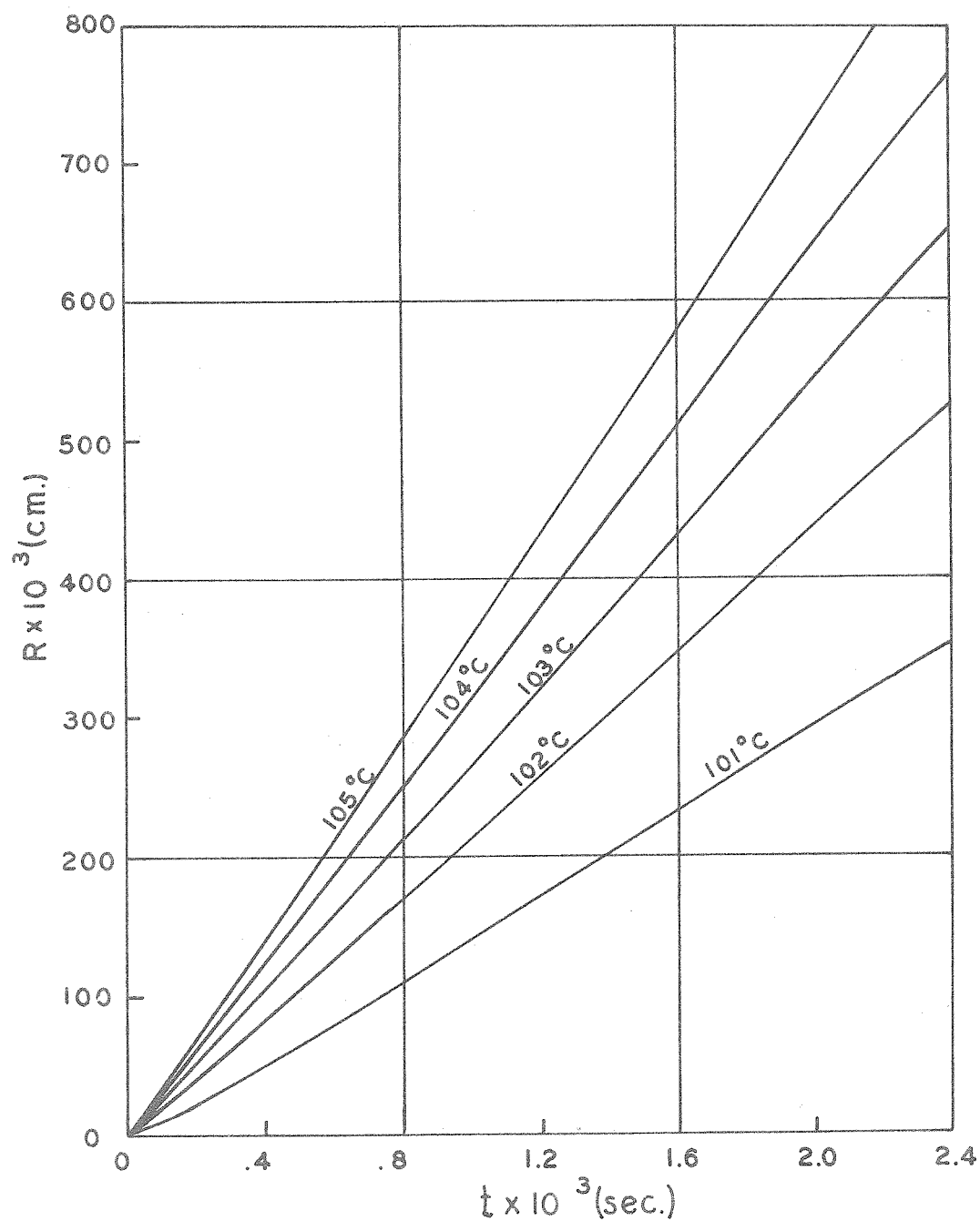


Fig. 6a - The actual radius R of the bubble is shown for various values of the water temperature T as a function of the time t , as obtained from Eq. (19).

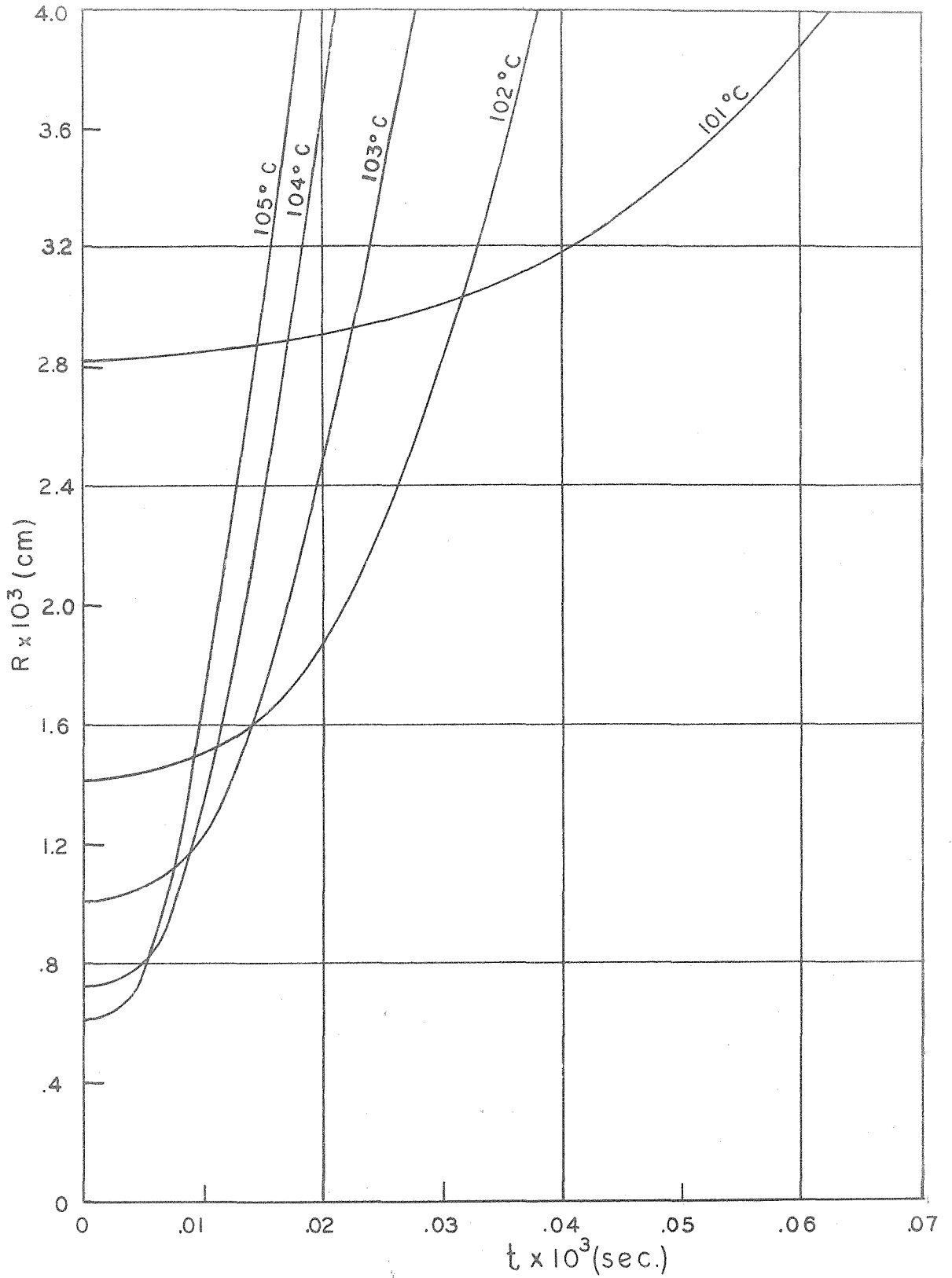


Fig. 6b - A detailed plot is shown of Fig. 6a near the region $R = 0$, $t = 0$.

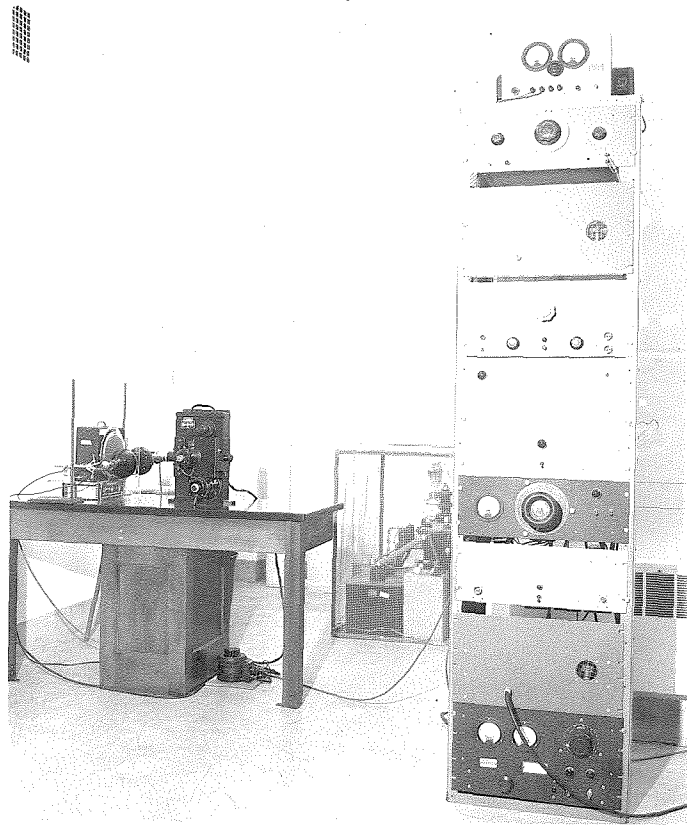


Fig. 7 - The upper figure shows the entire experimental setup of the electronic equipment, heat lamps, camera, and water beaker. The lower picture is a closeup of the camera, beaker, heat lamps, and flash lamp.

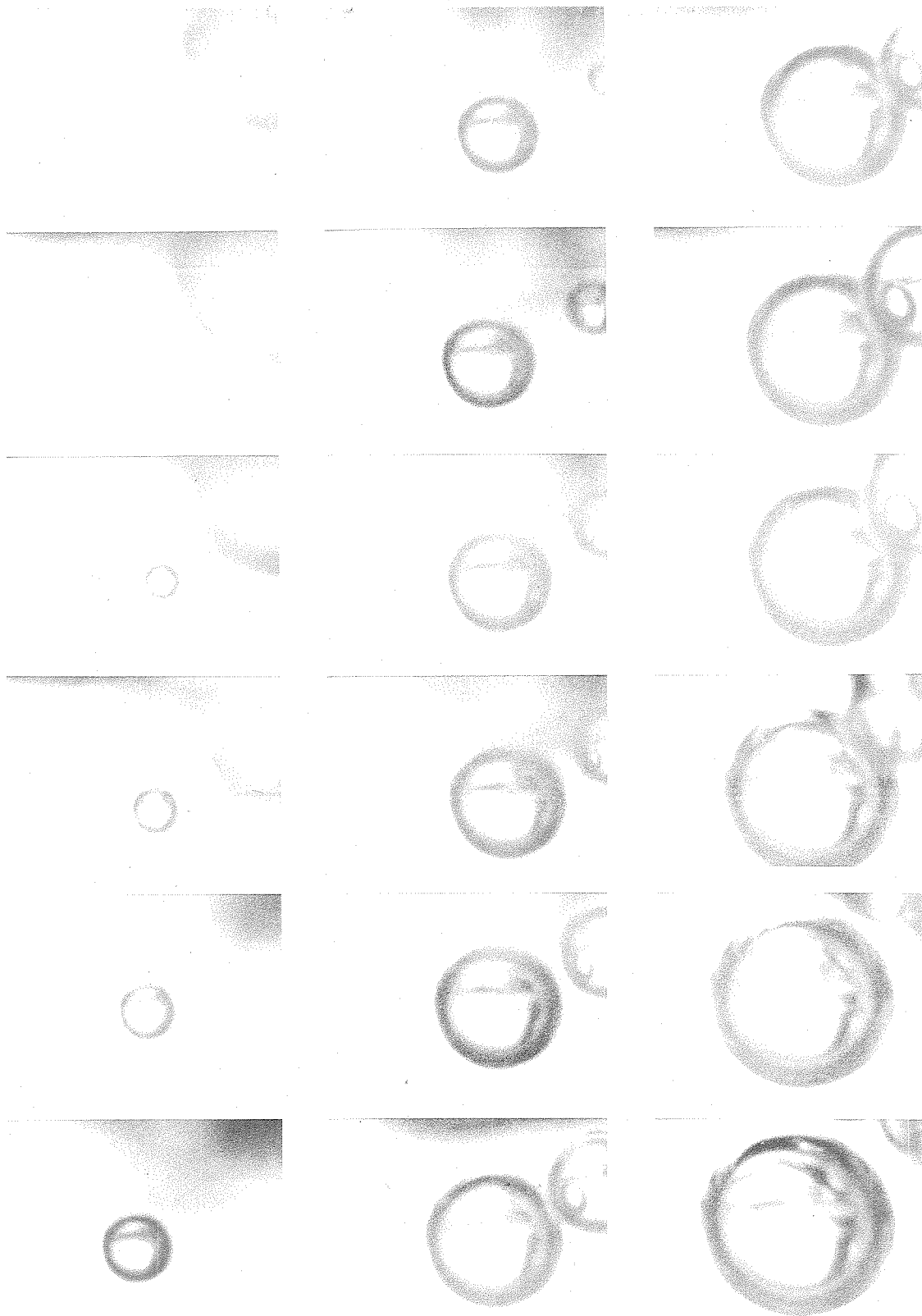


Fig. 8 - Photographic history of the rate of growth of bubble No. 9 ($T = 103.1^{\circ} \text{C}$). The time interval between successive pictures is .001 second. The top margin of each print is a reference point from which the translational motion of the bubble can be measured.

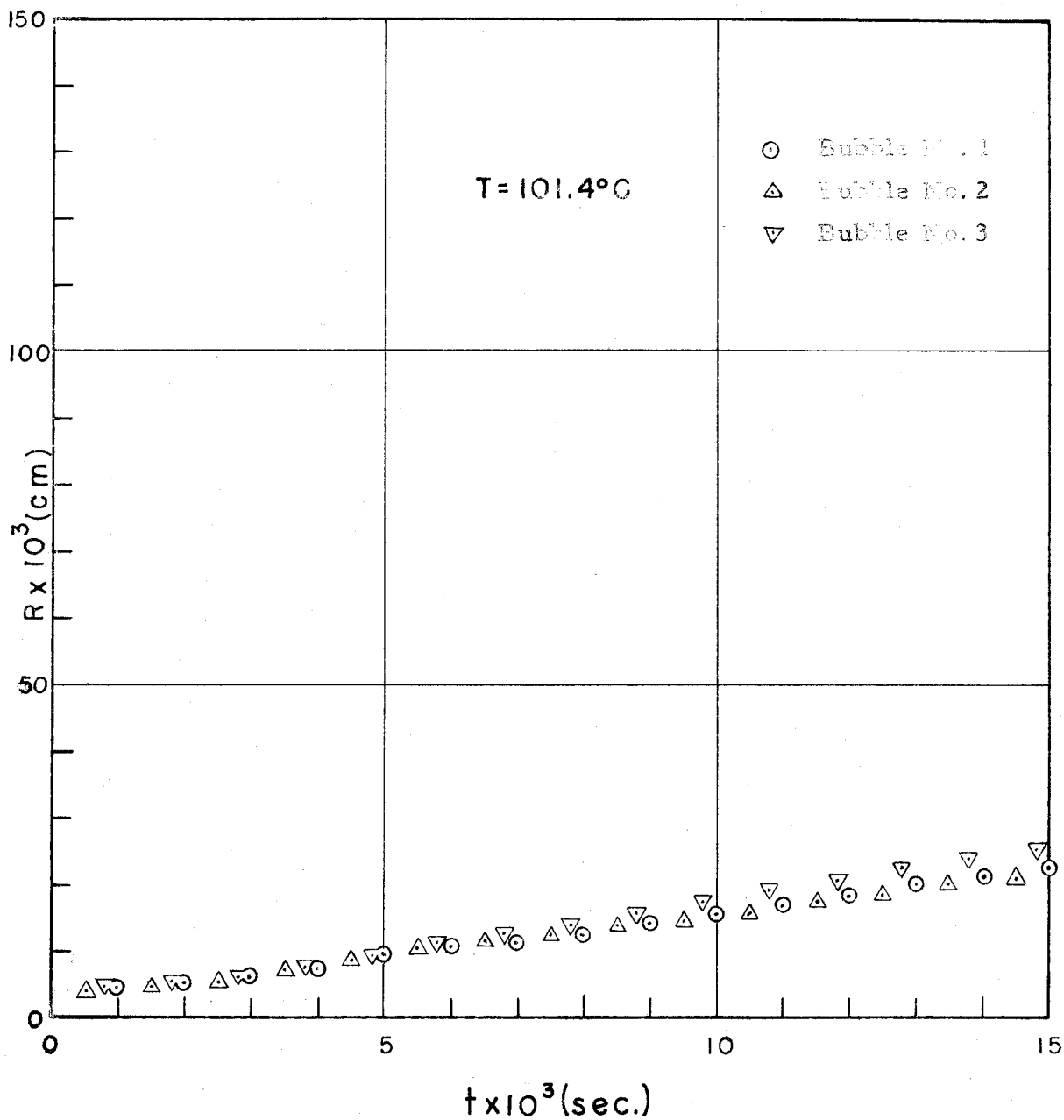


Fig. 9 - The radius of the bubble is shown as a function of the time for Bubbles Nos. 1, 2, and 3.

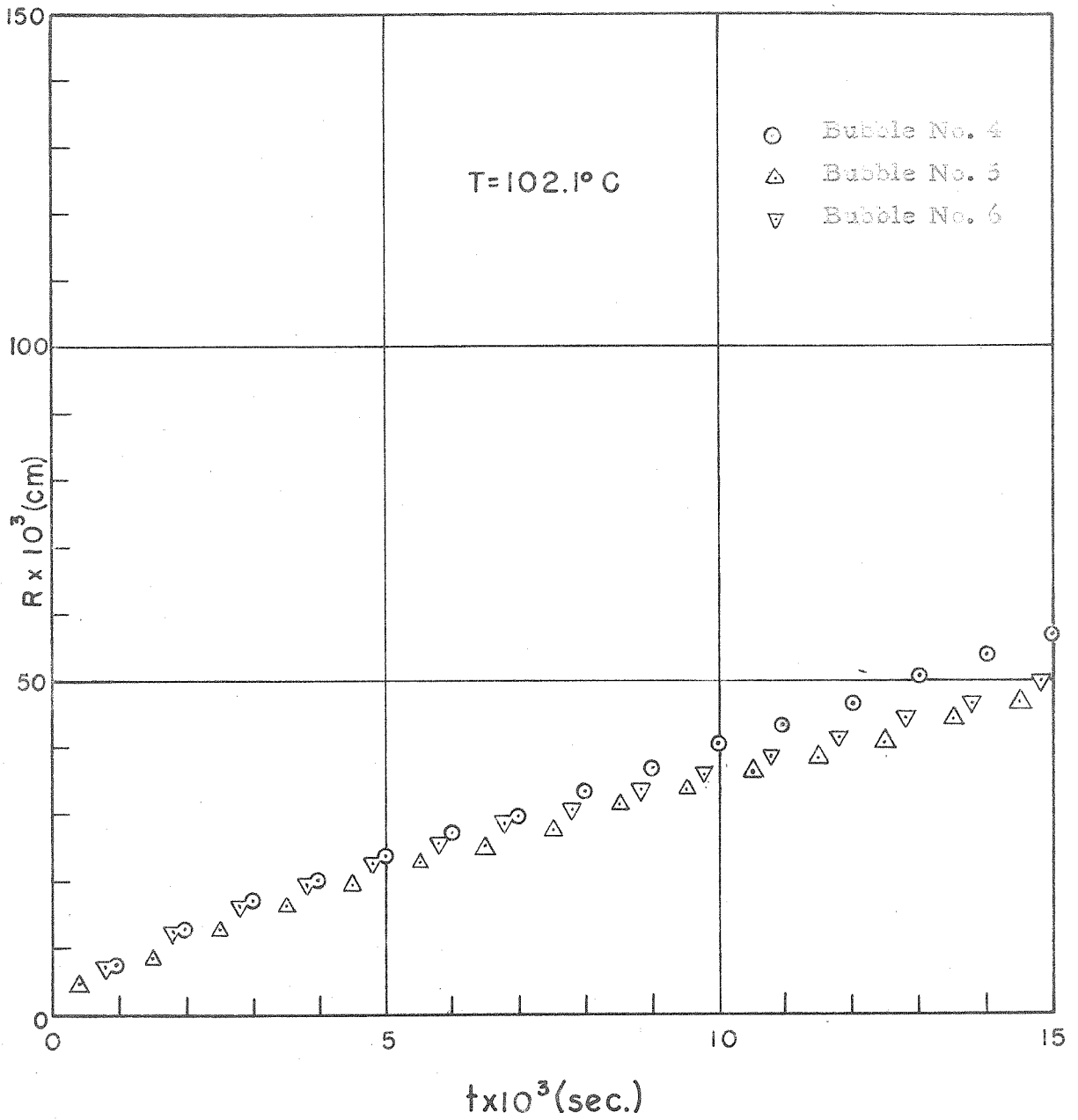


Fig. 10 - The radius of the bubble is shown as a function of the time for Bubbles Nos. 4, 5, and 6.

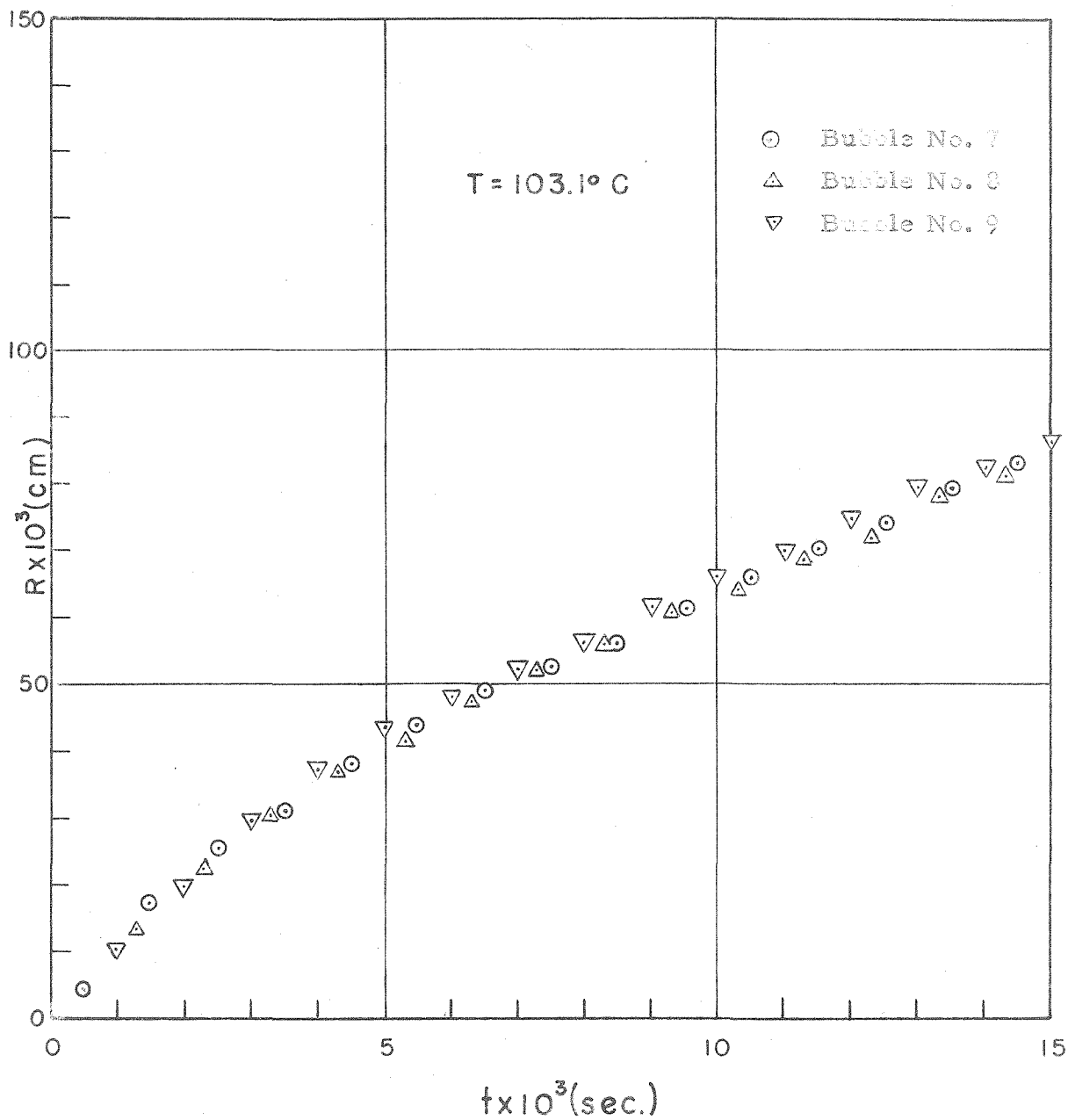


Fig. 11 - The radius of the bubble is shown as a function of the time for Bubbles Nos. 7, 8, and 9.

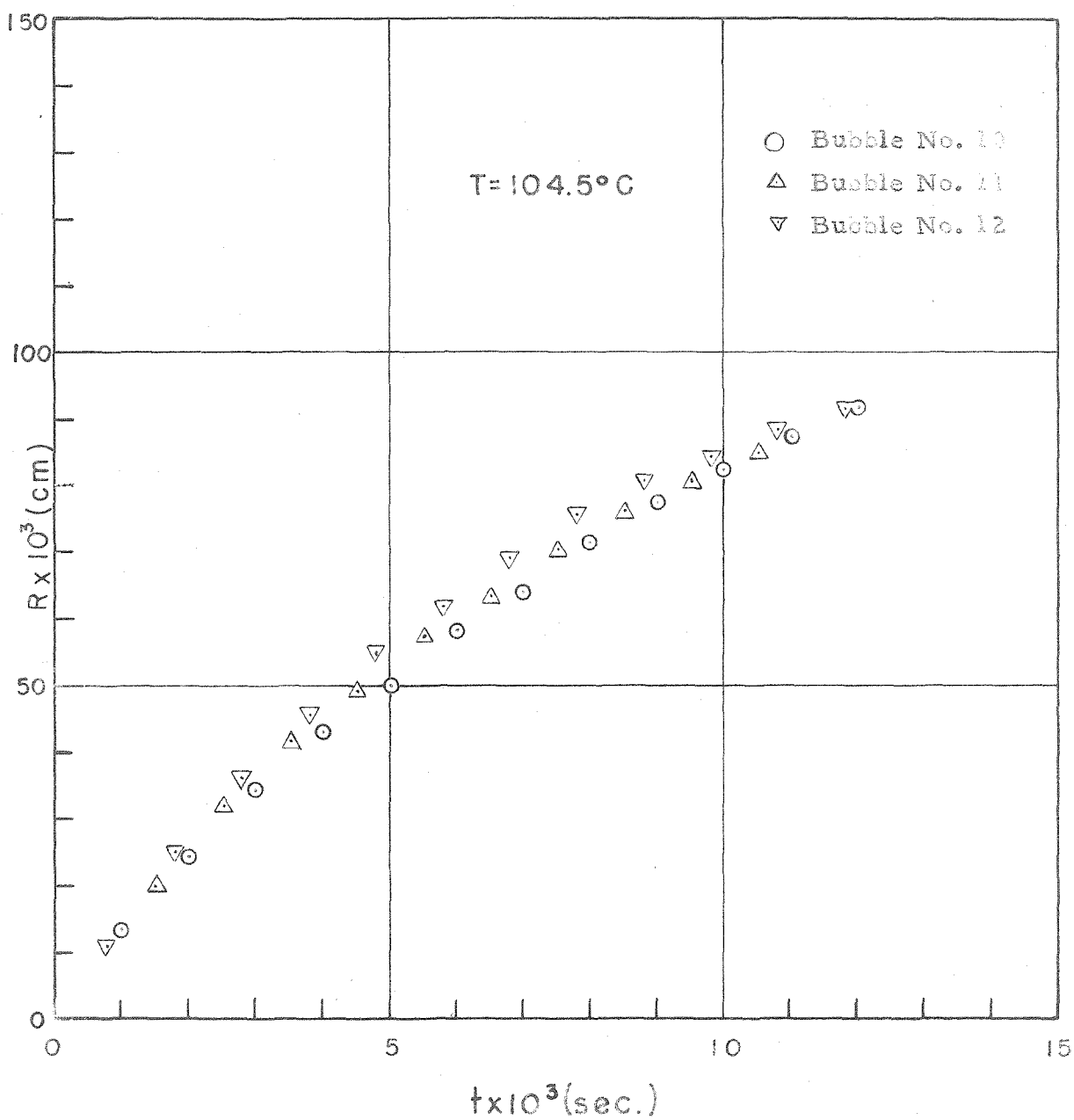


Fig. 12 - The radius of the bubble is shown as a function of the time for Bubbles Nos. 10, 11, and 12.

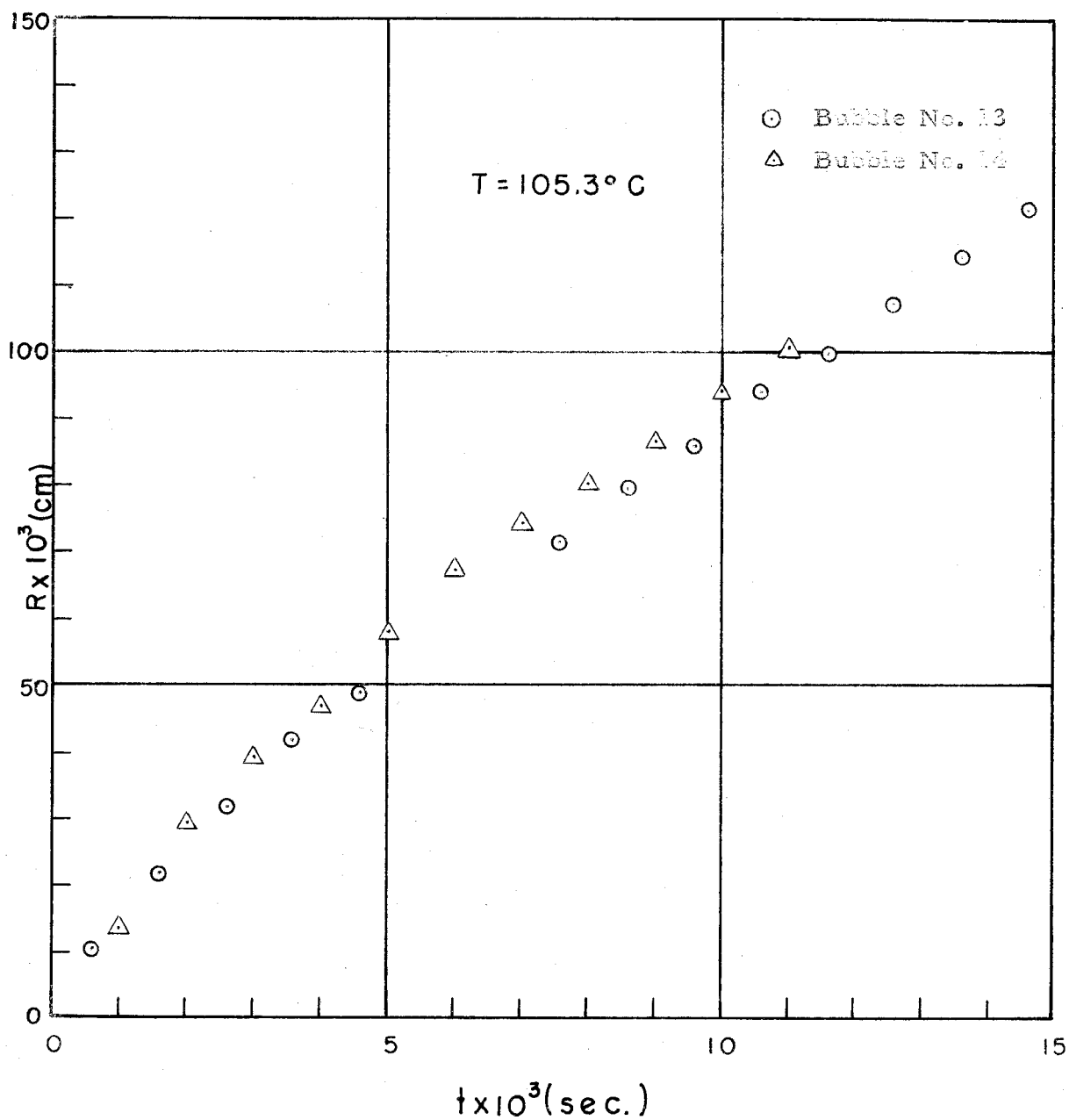


Fig. 13 - The radius of the bubble is shown as a function of the time for Bubbles Nos. 13 and 14. (The two points missing for Bubble No. 13 were the result of faulty negatives.)

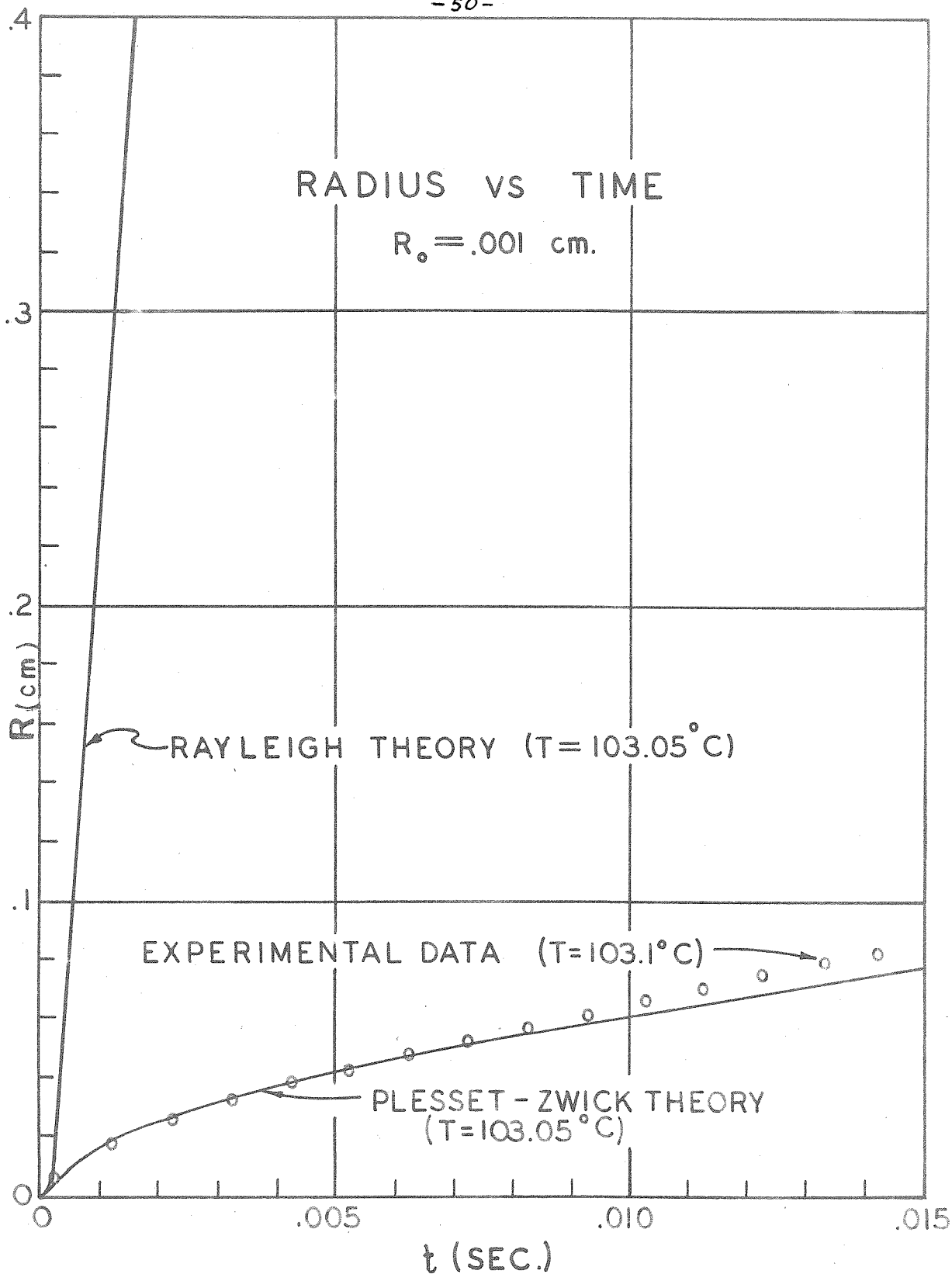


Fig. 14 - The bubble radius is shown as a function of time for a temperature of 103.1°C as obtained from experimental data (Bubble No. 7), the Rayleigh Theory, and the Plesset-Zwicky Theory.